

High Field Specific Heat of 2D Quantum Spin System $\text{SrCu}_2(\text{BO}_3)_2$

G.A. Jorge^{1,a}, R. Stern², M. Jaime¹, N. Harrison¹, J. Bonča^{3,4},

S. El Shawish⁴, C.D. Batista⁵, H.A. Dabkowska⁶, and B.D. Gaulin⁶

¹ MST-NHMFL, Los Alamos National Laboratory, Los Alamos, NM 87545, USA.

^a Also Departamento de Física, Universidad de Buenos Aires, Bs. As., Argentina

² National Institute of Chemical Physics & Biophysics (NICPB), Tallinn, Estonia.

³ Department of Physics, FMF University of Ljubljana and ⁴ J. Stefan Institute, Ljubljana, Slovenia

⁵ Theoretical Division, Los Alamos National Laboratory, Los Alamos, NM 87545, USA and

⁶ Department of Physics and Astronomy, McMaster University, Hamilton, ON, L8S 4C6, Canada

(Dated: January 19, 2004; Received textdate; Revised textdate; Accepted textdate; Published textdate)

We report measurements of the specific heat of the quantum spin liquid system $\text{SrCu}_2(\text{BO}_3)_2$ in continuous magnetic fields H of up to 33 T. The specific heat data, when combined with a finite temperature Lanczos diagonalization of the Shastry-Sutherland Hamiltonian, indicates the presence of a nearest neighbor Dzyaloshinsky-Moriya (DM) interaction that violates the crystal symmetry for $H = 0$. Moreover, the same DM interaction is required to explain the observed ESR lines for $H \parallel c$. These results indicate that spin-lattice coupling needs to be included in any realistic description of this system.

PACS numbers: 75.45.+j, 75.40.Cx, 05.30.Jp, 67.40.Db, 75.10.Jm

$\text{SrCu}_2(\text{BO}_3)_2$ is a quasi-two dimensional spin system with a singlet dimer ground state [1]. It is the only known realization of the Shastry-Sutherland model [2], and exhibits a sequence of magnetization plateaux at high magnetic fields [3, 4]. The unique behavior of this quantum spin liquid results from the interplay between two different fascinating aspects of strongly correlated spin systems: namely *geometrical frustration* and *strong quantum fluctuations*. The spin $s = 1/2$ Cu^{2+} ions that are responsible for the magnetism are grouped in dimers within planes of the tetragonal $\text{SrCu}_2(\text{BO}_3)_2$ unit cell, with respective intra-dimer or nearest neighbor (nn) and inter-dimer or next nearest neighbor (nnn) separations of 2.9 Å and 5.1 Å. The coupling constants are estimated to be $J \sim 80$ K for nn and $J' \sim 50$ K for nnn [5]. The geometrical frustration of the spin-lattice leads to very localized triplet excitations that have a tendency to crystallize at high magnetic fields. This occurs when the concentration of triplets reaches certain values that are commensurate with the underlying lattice, becoming incompressible upon formation of a gapped structure. The magnetization plateaux at $H_{p1} = 27$ T, $H_{p2} = 35$ T and $H_{p3} = 42$ T are a direct consequence of spin superstructures forming at triplet concentrations 1/8, 1/4 and 1/3 respectively.

Recent ESR experiments [6, 7, 8] revealed the spin triplet excitation energy to decrease linearly with increasing magnetic field, extrapolating to zero at a field value ($H = 22$ T) very close to H_{p1} . However, on approaching H_{p1} , the experimental ESR data deviates from this linear extrapolation, indicating a level anti-crossing between the first triplet excitation and the ground state. The anti-crossing implies some mixing between two states with different magnetization M_z along the tetragonal c -axis. This observation cannot be explained by the $U(1)$ invariant models (which are symmetric under rotations around the c -axis) proposed in previous works, for which M_z is a good quantum number.

In this letter we argue that an intra-dimer Dzyaloshinsky-Moriya (DM) interaction, which violates the observed crystal

symmetry at $100\text{K} \leq T \leq 395\text{K}$ [9], is required to explain the low temperature specific heat of $\text{SrCu}_2(\text{BO}_3)_2$ in magnetic fields $H > 18$ T. We also show that this interaction gives rise to the ESR transitions between the ground state and the single triplet excitations that are observed for $H \parallel c$ [6, 7, 8]. These results suggest that there is a structural phase transition at low temperatures that lowers the crystal symmetry. Such a transition could be driven by a strong spin-lattice interaction that would be a relevant ingredient to explain the magnetization plateaux which are observed in this system.

The single crystal sample of $\text{SrCu}_2(\text{BO}_3)_2$ used in this study was grown by the floating zone technique. Stoichiometric amounts of CuO , SrCO_3 and B_2O_3 were mixed, pre-annealed, and then annealed at 870 °C. Finally, the powder was reground, pelletized and annealed in O_2 several times. Rods were formed by hydrostatic pressing and the growth was performed in a Crystal System Optical Furnace at a growth speed of 0.25mm/h in O_2 . No additional flux was applied [10]. The measurements of the specific heat $C(T, H)$ of $\text{SrCu}_2(\text{BO}_3)_2$ in continuous magnetic fields up to 33 T were performed on two oriented single crystal pieces of 12.34 mg and 13.92 mg. Both were measured with H applied along the tetragonal c -axis and within the ab planes. A calorimeter made of plastic materials and silicon was used, employing a thermal relaxation time technique optimized for rapid data acquisition [11, 12]. The magnetization M_z of a piece of sample of approximate dimensions $1.5 \times 0.9 \times 0.5$ mm³ was measured as a function of field using a sample-extraction magnetometer in a 400 ms, 45 T pulsed magnet provided by the National High Magnetic Field Laboratory at Los Alamos [13]. The small size of the sample, placed in good thermal contact with liquid ^3He or ^4He below $T = 4$ K, combined with the relatively slow field sweep of the magnet helped minimize magnetocaloric effects so as to achieve an isothermal experiment [14]. For characterization purposes, supplementary M_z versus temperature T measurements and specific

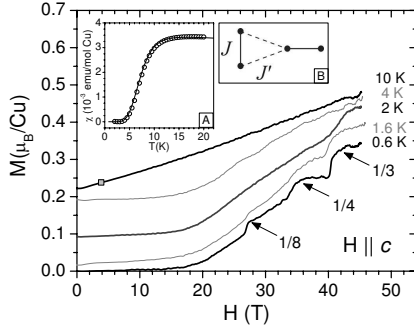


FIG. 1: Magnetization vs field for $\text{SrCu}_2(\text{BO}_3)_2$ at different temperatures between 0.6 K and 10 K, as indicated, reveal a gradual evolution of the magnetization plateaux. The square point on the 10 K curve was used to compare with SQUID magnetometer data in order to obtain the magnetization units. Inset A: Magnetic susceptibility measured at $H = 4$ T in a SQUID magnetometer (circles). The solid line is the susceptibility calculated with the FTL method. Inset B: Two copper dimers in the CuBO_3 plane where the coupling constants J (nn) and J' (nnn) are indicated.

heat measurements were made at lower fields using a commercial Quantum DesignTM MPMS (SQUID magnetometer). Meanwhile, numerical simulations of the Shastry-Sutherland model, with which the experimental data are compared, were performed on a 20-site square lattice using the finite temperature Lanczos (FTL) method [15, 16, 17].

To describe the present system, we consider the following Heisenberg Hamiltonian on a Shastry-Sutherland lattice [2]:

$$H_s = J \sum_{\langle i,j \rangle} \mathbf{S}_i \cdot \mathbf{S}_j + J' \sum_{\langle i,j \rangle'} \mathbf{S}_i \cdot \mathbf{S}_j + \sum_{\langle i \rightarrow j \rangle} \mathbf{D} \cdot (\mathbf{S}_i \times \mathbf{S}_j) + \sum_{\langle i \rightarrow j \rangle'} \mathbf{D}' \cdot (\mathbf{S}_i \times \mathbf{S}_j). \quad (1)$$

Here, $\langle i, j \rangle$ and $\langle i, j \rangle'$ indicate that \mathbf{i} and \mathbf{j} are *nn* and *nnn* respectively. The Hamiltonian includes *nn* (\mathbf{D}) and *nnn* (\mathbf{D}') DM interactions. The arrows indicate that the corresponding bonds have a particular orientation. The quantization axis \hat{z} is parallel to the *c*-axis. The *nnn* DM interaction has already been considered in previous papers [18] to explain the position of the single triplet excitations observed with ESR [6, 8], far infra-red [19] and inelastic neutron scattering measurements [20]. From the splitting between the two single-triplet excitations at $\mathbf{q} = \mathbf{0}$, the \mathbf{D}' is estimated to be: $\mathbf{D}' = 2.1 \text{ K}\hat{z}$. The orientation of the *nnn* bonds is given in Ref. [18]. According to the crystal symmetry [9], the *xy* component of \mathbf{D} is perpendicular to the corresponding dimer. However, as is explained below, a non-zero *z* component of \mathbf{D} , which is not allowed by the observed crystal symmetry at high temperatures ($100 \text{ K} \leq T \leq 395 \text{ K}$), is required to explain the specific heat and the ESR data as a function of the applied field H .

Figure 1 shows the magnetization $M_z(H)$ measured as a function of magnetic field, in units of μ_B/Cu determined upon cross-calibration with SQUID magnetometry data. In addition to the plateaux already mentioned, there is a small ex-

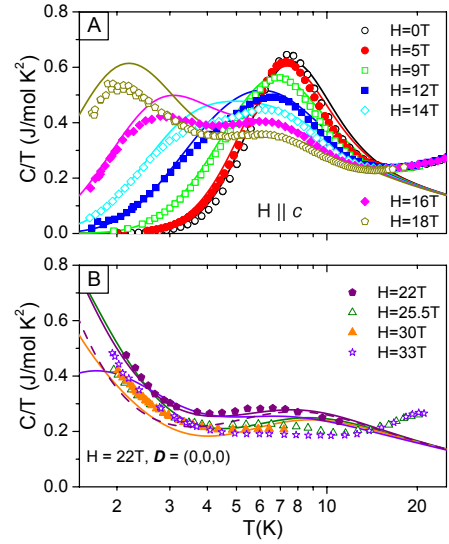


FIG. 2: Measured specific heat divided by T (symbols) vs. T compared with the calculated one for the Hamiltonian of Eq. 1 (solid lines) for the magnetic field along the *c*-axis: A) $0 \leq H \leq 18$ T and B) $20 \leq H \leq 33$ T. The parameters are the same ones used to compute the magnetic susceptibility. The dashed line is the calculated C/T for $\mathbf{D} = \mathbf{0}$ and $H = 22$ T.

cess contribution to M_z identified in our data over the entire field range. This additional source of magnetization has been observed before in SQUID magnetometry data [3], although for reasons which are unknown to us, it is absent in published pulsed magnetic field data. For our samples, both SQUID magnetometry data and low field pulsed magnetic field data evidence a finite excess susceptibility of approximately $0.115 \times 10^{-3} \text{ emu/mol Cu}$, probably due to crystalline defects. Good agreement with the expected magnetization values at the plateaux is obtained by subtracting this value. Better agreement is obtained by subtracting a scaled Brillouin function with an initial slope of $0.14 \times 10^{-3} \text{ emu/mol Cu}$ and a characteristic temperature of 5 K (see Fig. 1). After either of these subtractions, there remains a finite value of M_z at very low temperatures and magnetic fields that increases linearly with H .

In the inset of Fig. 1 we compare the measured magnetic susceptibility $\chi(T)$ (after subtracting a small constant value of $0.14 \times 10^{-3} \text{ emu/mol Cu}$) and the curve obtained with the FTL method that is described below. We get an excellent agreement for: $J = 74 \text{ K}$, $J' = 0.62J$, $\mathbf{D} = (2.2 \text{ K}, \pm 2.2 \text{ K}, 5.2 \text{ K})$ (the sign is different for each dimer in the unit cell), $\mathbf{D}' = (0, 0, 2.2 \text{ K})$. The values of the *g*-factors, $g_{\parallel} = 2.15$ and $g_{\perp} = 2.08$, have been obtained from a comparison between our theoretical calculations [21] (see Fig. 4) and the ESR spectra [6, 8].

In Fig. 2, we show the specific heat divided by temperature, $C(T, H)/T$, for different values of the magnetic field applied along the *c*-axis. The primary feature in the low temperature specific heat is a broad anomaly centered at $T = 8.5 \text{ K}$ that is gradually depressed by increasing H . This anomaly has been attributed [22] to $S_z = 0$ dimer excitations. Here, how-

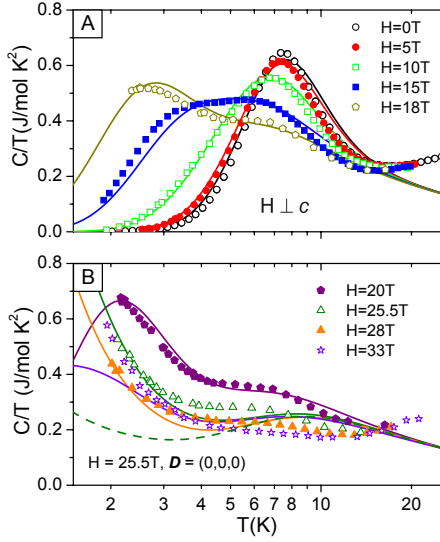


FIG. 3: Measured specific heat divided by T (symbols) vs. T compared with the calculated one for the Hamiltonian of Eq. 1 (solid lines) for the magnetic field perpendicular to the c -axis: A) $0 \leq H \leq 18$ T and B) $22 \leq H \leq 33$ T. The parameters are the same ones used to compute the magnetic susceptibility. The dashed line is the calculated C/T for $\mathbf{D} = 0$ and $H = 25.5$ T.

ever, we observe a small shift in temperature as function of H , indicating the involvement of states with $S_z \neq 0$. For $H \geq 12$ T, a second anomaly develops at lower temperatures, which we attribute to single-triplet excitations situated 3 meV above the ground state in zero field. The Zeeman interaction causes this triplet states to move to lower energies with increasing H . Figure 3 shows similar results for $H \perp c$.

In Figs. 2 and 3, we also compare the experimental results with the results of a numerical simulation of $C(T, H)/T$ made using the FTL method [15, 16]. This method is based on the Lanczos procedure of exact diagonalization, and uses a random sampling over initial wave functions specially adapted for calculation of thermodynamic properties. All the results were computed on a tilted square lattice of $N = 20$ sites. There are many advantages of this method over the conventional Quantum Monte Carlo (QMC) methods, which are as follows: first, the minus-sign problem that usually appears in QMC calculations of frustrated spin systems is absent; second, the method connects the high- and low-temperature regimes in a continuous fashion, enabling the entropy density and specific heat (per unit cell) to be computed as expectation values (*i.e.* $s = k_B \ln Z/N + \langle H \rangle / NT$, where Z is the statistical sum). The specific heat is then given by $C_V = T(\partial s / \partial T) = k_B(\langle H^2 \rangle - \langle H \rangle^2) / NT^2$. The main limitation to the validity of the results originates from finite-size effects which occur when $T < T_{fs}$. The actual value of T_{fs} depends strongly on the particular physical properties of the system. For gapless systems, T_{fs} can be defined by way of the thermodynamic sum $\tilde{Z}(T) = \text{Tr} \exp(-(H - E_0)/T)$, on condition that $\tilde{Z}(T_{fs}) = Z^* \gg 1$ [16]. In the present case, this condition can be relaxed ($Z^* > 1$) owing to the existence

of a gap in the excitation spectrum when $J'/J < 0.7$ and to the almost localized nature of the lowest excited states - triplet excitations. By comparing results obtained on two different systems with $N = 16$ and $N = 20$ sites, we estimate $T_{fs} < 1$ K.

For $H < 18$ T, the agreement between theory and experiment is very good, regardless of the inclusion of the nn DM interaction. Finite size effects are also very small, for $H < 18$ T, due to the localized nature of the single-triplet excitations [20]. When H approaches 22 T for $H \parallel c$ (or 25 T for $H \perp c$), however, the inclusion of this interaction is required to explain the measured $C(T, H)/T$ at low temperatures. For $H \parallel c$, this is explained by the fact that \mathbf{D} is the only interaction that violates the conservation of M_z , by mixing the $M_z = 0$ singlet ground state of $H(\mathbf{D} = 0)$ with the single-triplet excited state with $M_z = \pm 1$. This mixing becomes effective only when the energy difference between both levels is comparable to $|\mathbf{D}|$. For $H \perp c$, the same type of mixing is produced by the z -component of \mathbf{D} . In other words, the level crossing that would occur in absence of the DM interactions is replaced by level anti-crossing. This can be seen in Figs. 2b and 3b where we also show the calculated C/T for $\mathbf{D} = 0$ and $H = 22$ T ($H = 25.5$ T) for $H \parallel c$ ($H \perp c$). In absence of the DM interactions, the level crossing generates a peak of C/T at $T = 0$ which is not consistent with the experiment. In contrast, the level anti-crossing moves this peak to higher temperatures in agreement with the experimental data. The anti-crossing occurs for different values of H in the different field orientations due to the anisotropy of the g -factor and the fact that \mathbf{D} is parallel to the c axis [6, 8]. At high temperatures ($T > 20$ K), the specific heat data deviates from the theoretical prediction owing to significant phonon contributions.

For $T \sim 10$ K and fields $H > 20$ T, there are small deviations between the experimental curves and the calculations, which can be attributed to the inter planar antiferromagnetic interaction $J''/J \sim 0.21$ that becomes relevant when the concentration of triplet excitations increases.

The components of the nn DM interaction are constrained by the crystal symmetry at low temperatures [9]. According to this symmetry, the z -component of \mathbf{D} must be zero. Although a non-zero DM vector of the form $(d, \pm d, 0)$ improves considerably the agreement between experiment and theory for $H \parallel c$, it does not reproduce our experimental data in the proximity of $H_{p1} = 27$ T for $H \perp c$. Ultrasonic experiments [24] indicate that in this region the lattice gets strongly distorted by the application of the magnetic field. We speculate that this lattice distortion increases the z -component of the DM vector to lower the magnetic energy (it increases the level anti-crossing).

This speculation is further supported by the measured ESR spectrum for $H \parallel c$ [6, 8]. We show the ESR spectrum as a function of H for $D_z = 5.2$ (Fig. 4a) and $D_z = 0$ K (Fig. 4b) calculated with the Lanczos method [21]. More specifically, we are computing the dynamical susceptibility along the direction perpendicular to the applied field using the method introduced in Ref. [23]. As it is pointed out in Ref. [7],

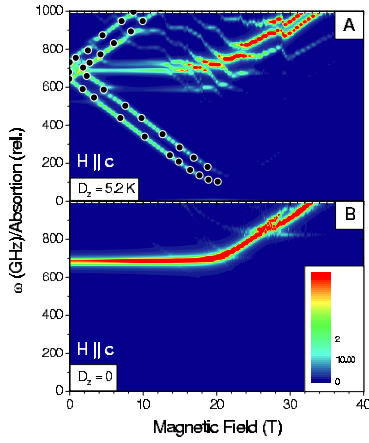


FIG. 4: Contour color plot for the ESR spectrum for $H||c$ calculated with the Lanczos method in a 20 sites cluster for a) $D_z = 5.2$ K and b) $D_z = 0$. The values of the other parameters are the same ones used to compute the magnetic susceptibility. The experimental data points in a) are from Cepas et al., [6].

the observed ESR transitions between the ground state and the single-triplet excitations are not allowed by the observed crystal symmetry at $H = 0$ [9]. In Fig. 4a we show that these ESR transitions can be explained with a non-zero value of D_z , while the corresponding ESR lines are not present if $D_z = 0$ (Fig. 4b). None of the other components of \mathbf{D} or \mathbf{D}' can reproduce these ESR lines. Based on these observations, we propose that the crystal symmetry is lowered at low temperatures due to a strong spin-lattice interaction. Since the lattice distortion depends on the applied field [24], we expect D_z to be an increasing function of H (although we used a constant value $D_z = 5.2$ K for our calculation).

With the exception of \mathbf{D} , all other physical parameters used in the model were determined from previous experiments. The values of $g_{||}$ and g_{\perp} are obtained from the ESR spectra [6, 8]. By including \mathbf{D} , however, we are able to account simultaneously for the ESR spectra as a function of the applied field (see also Ref. [21]), the temperature dependence of the susceptibility, and the low temperature specific heat data for $H \gtrsim 18$ T.

In summary, we have measured the specific heat as a function of temperature in continuous magnetic fields up to 33 T. An excellent fit to the $C(T, H)/T$ data for both field orientations is obtained for a nn exchange constant $J = 74$ K, a ratio $J'/J = 0.62$, a nn Dzyaloshinsky-Moriya interaction

constant $|\mathbf{D}| = 6.1$ K, and a nnn Dzyaloshinsky-Moriya interaction constant $|\mathbf{D}'| = 2.2$ K. A non-zero value of D_z , that is not allowed by the observed crystal symmetry at $H = 0$, is required to explain both the specific heat data for $H \gtrsim 18$ T and the observed ESR [6, 8] spectrum for $H||c$. This suggests that a lattice distortion that lowers the crystal symmetry is induced at low temperatures. A more detailed comparison between the calculated ESR spectrum and the experiment will be presented elsewhere [21].

This work was sponsored by the US DOE under contract W-7405-ENG-36. R.S. was supported by the National High Magnetic Field Laboratory and Estonian Science Foundation grant No.4931. J.B. acknowledges the financial support of Slovene MESS. Work performed at the National High Magnetic Field Laboratory is supported by the National Science Foundation (DMR90-16241), the Department of Energy and the State of Florida.

-
- [1] R.W. Smith and D.A. Kesler, J. Solid State Chem. **93**, 430 (1991).
 - [2] B.S. Shastry and B. Sutherland, Physica B **108**, 1069 (1981).
 - [3] H. Kageyama et al., Phys. Rev. Lett. **82**, 3168 (1999).
 - [4] K. Onizuka et al., J. Phys. Soc. Jap. **69**, 1016 (2000).
 - [5] S. Miyahara and K. Ueda, Phys. Rev. Lett. **82**, 3701 (1999).
 - [6] O. Cépas et al., Phys. Rev. Lett. **87**, 167205 (2001).
 - [7] O. Cépas and T. Ziman, cond-mat/0207191.
 - [8] H. Nojiri et al., cond-mat/0212479
 - [9] K. Sparta et al., Eur. Phys. J. **19**, 507 (2001).
 - [10] H. Dabkowska et al., to be published.
 - [11] M. Jaime et al., Nature **405**, 160 (2000).
 - [12] G.A. Jorge et al., unpublished
 - [13] G.A. Jorge et al., to be published
 - [14] M. Jaime et al., Phys. Rev. Lett. **89**, 287201 (2002).
 - [15] J. Jaklič and P. Prelovšek, Phys. Rev. Lett. **77**, 892 (1996); Phys. Rev. B **49**, 5065 (1994).
 - [16] J. Jaklič and P. Prelovšek, Adv. Phys. **49**, 1 (2000).
 - [17] J. Bonča and P. Prelovšek, Phys. Rev. B **67**, 085103 (2002).
 - [18] S. Miyahara and K. Ueda, J. Phys.: Condens. Matter **15**, R327 (2003).
 - [19] T. Rößm et al., Phys. Rev. **B61**, 14342 (2000).
 - [20] H. Kageyama, et al., Phys. Rev. Lett. **84**, 5876 (2000).
 - [21] J. Bonča, S. El Shawish and C. D. Batista, preprint.
 - [22] M. Hofmann et al., Phys. Rev. Lett. **87**, 047202 (2002).
 - [23] E. R. Gagliano and C. A. Balseiro, Phys. Rev. Lett. **59**, 2999 (1987).
 - [24] S. Zherlitsyn et al., Phys. Rev. **B62**, R6097 (2000).